Viero et al., http://www.jcb.org/cgi/content/full/jcb.201406040/DC1

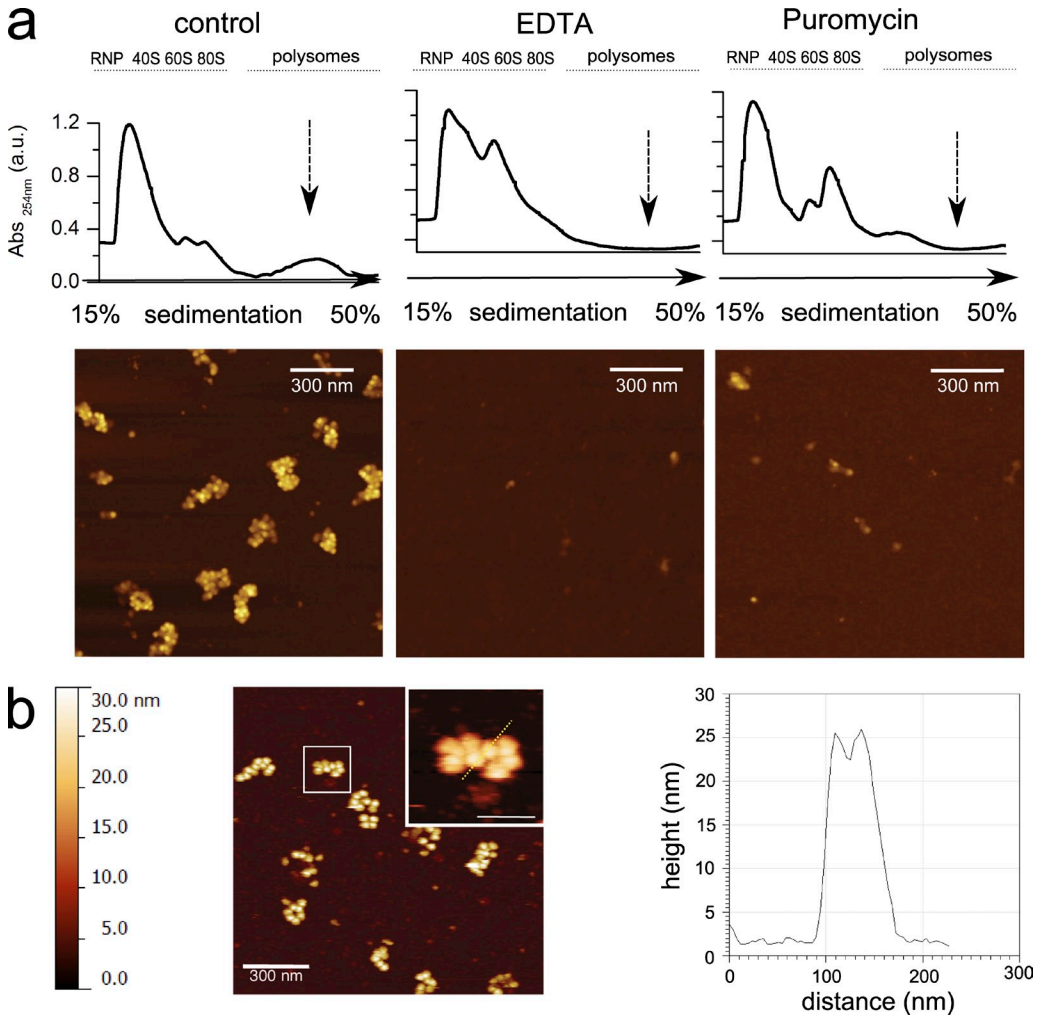

Figure S1. **Controls of AFM imaging: ribosome assemblies disappear after EDTA and puromycin treatments and display the expected height when measured in liquid.** (a) Polysome profiles of control and EDTA- and puromycin-treated cells obtained in a concave 15–50% sucrose gradient read by UV absorption at 254 nm. In the bottom panels, the fractions corresponding to HMW polysomes (see arrows) were analyzed by AFM. Z-scale 24 nm. Negative controls for polysome formation were run as follows: (1) the lysate was supplemented with 100 mM EDTA before the sucrose gradient separation of polysomes, and (2) the cells were incubated with 100 µg/ml puromycin for 10 min before harvesting the lysate. Each experiment was performed twice, and the images are representative examples of at least five acquisitions. (b, left) Typical AFM image of HMW polysomes acquired liquid. The image shown is from a single representative experiment out of six repeats. In the inset, an example of a magnified polysome is shown (bar, 100 nm). (right) The cross-section profile through two adjacent ribosomes is shown (dashed yellow line in the inset magnification).

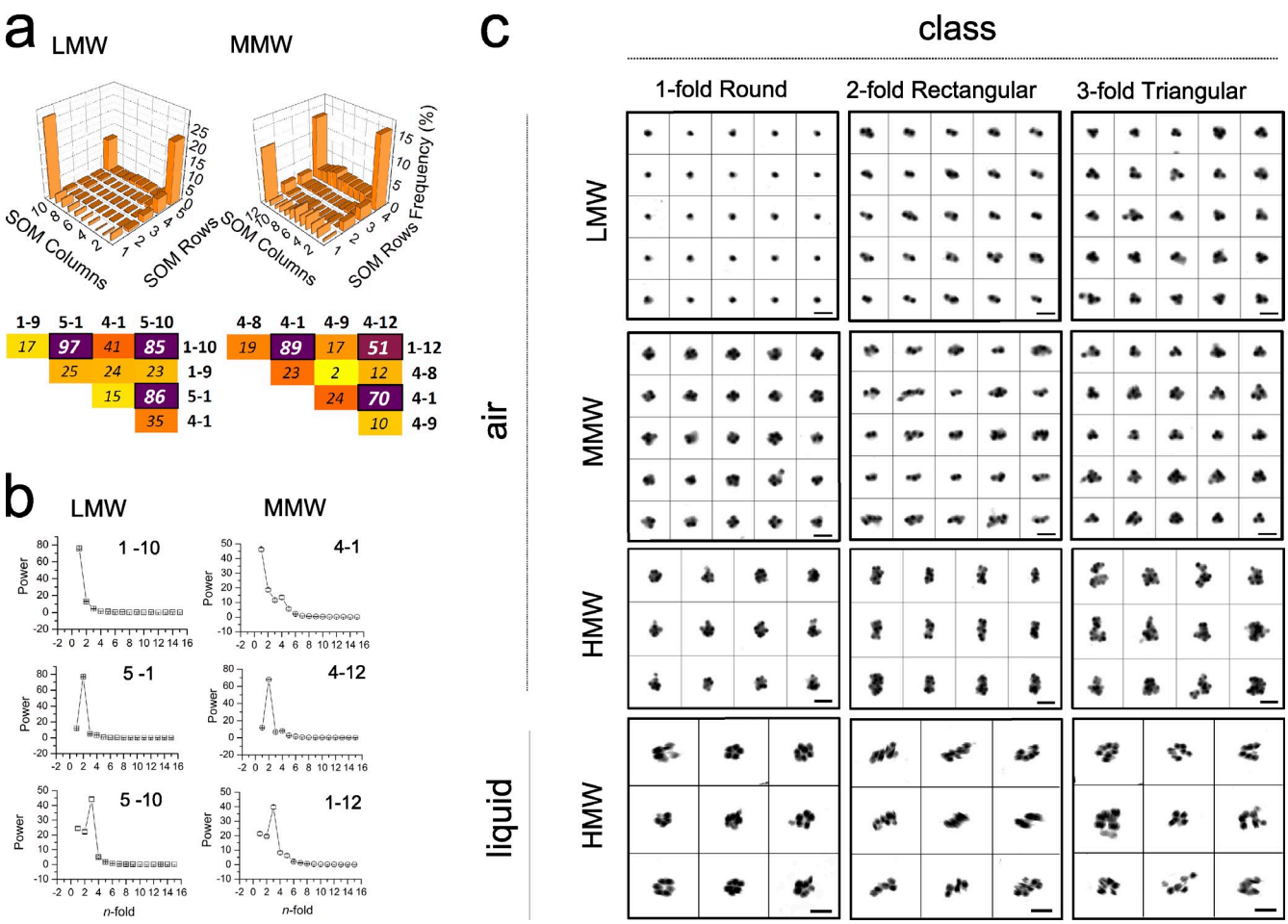

Figure S2. **Classification of LMW, MMW, and HMW polysomes in air and HMW polysomes in liquid by KerDenSOM maps.** Image classification was used to sort the population of images into clusters that are characterized by similar rotational symmetry. (a) Each set of images obtained for LMW and MMW polysomes was used for RSC that finds structural similarities in the data. The SOM obtained from the rotational classification is formed by slots of images displaying similar folds of symmetry. This classification method produces a regular low-dimensional grid, the so-called SOM. Frequency of objects assigned to a class after rotational classification for LMW and MMW samples (top) is shown. Each slot within the SOM is identified by a code number that describes its position as column-row (i.e., 1-1 indicates the slot in the top left corner of the SOM). Note that the position of classes with the same rotational properties in each KerDenSOM matrix is not the same for LMW, MMW, and HMW cases. In the bottom panel, the top MMD values are displayed as heat maps. The number of objects under classification is 544 and 560 LMW and MMW samples, respectively. (b) Rotational power spectra for the most populated SOM classes of LMW and MMW polysomes (mean ± SEM is displayed). (c) Galleries of polysomes belonging to the three classes identified by RSC. Images belonging to the most populated slots in each KerDenSOM matrix were isolated, and the corresponding galleries are reported here for LMW, MMW, and HMW fractions. The number of polysomes acquired in liquid and under classification is 648, and the others are 544, 560, and 674 for LMW, MMW, and HMW polysomes, respectively. Bars, 100 nm.

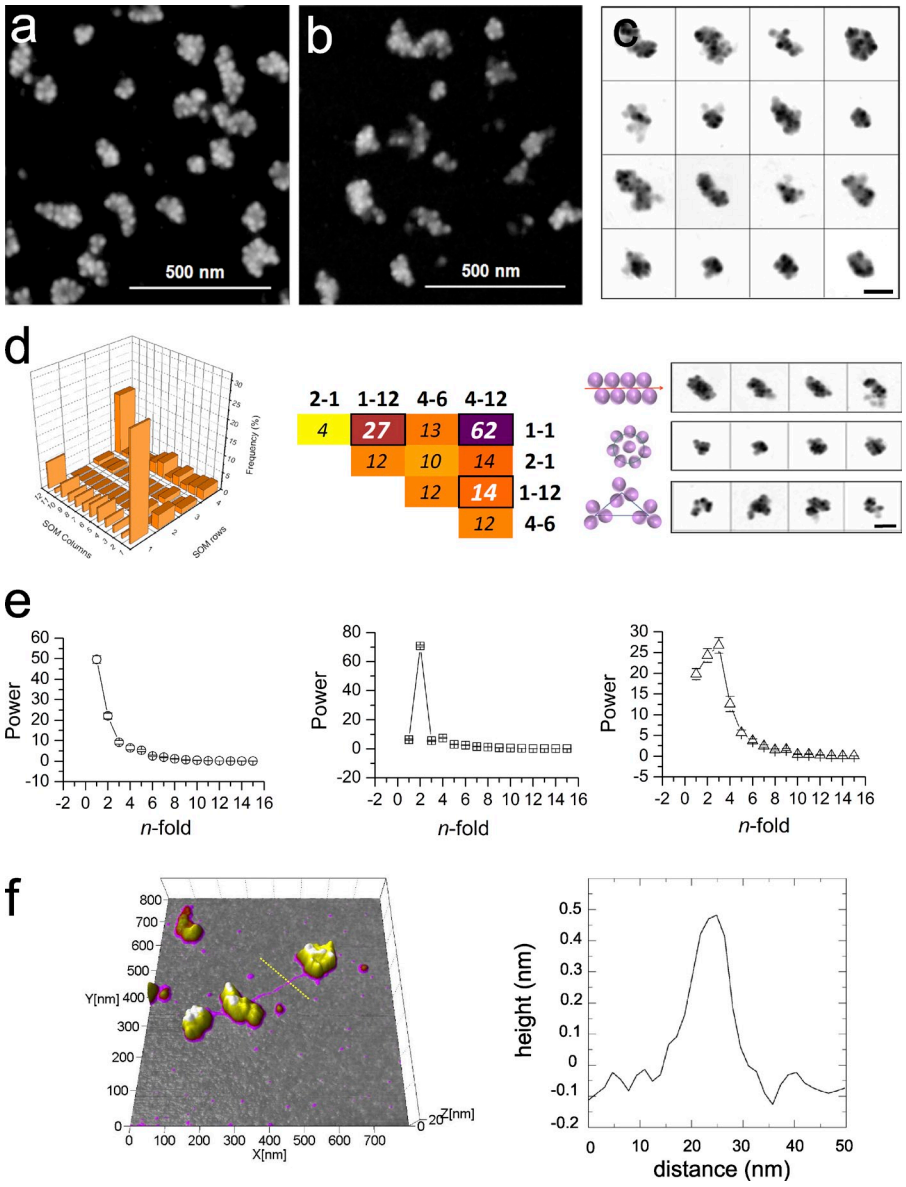

Figure S3. **AFM characterization and RSC of the HMW polysome fraction after GraFix.** We used the GraFix method that can be used to control for the dropping-off of ribosomes from the polysome. This method takes advantage of mild cross-linking conditions in combination with analytical centrifugation in sucrose gradients. In particular, we performed the classical sucrose gradient fractionation of cellular lysates in the presence of a PFA gradient (top–bottom 0–0.01%). (a) Images of polysomes without PFA cross-linking during the sucrose gradient fractionation were compared with a paradigmatic image of polysomes after GraFix. (b) GraFix HMW polysome images were then run through RSC. (c) Gallery of GraFix HMW polysomes after translational and rotational alignment (287 objects). (d) Frequency of objects classified by RSC. Three main classes are found. The top scoring inter-class differences calculated by MMD are plotted in heat map format in the middle panel. A gallery of objects belonging to the three main classes identified is shown in the right panel. (c and d) Bars, 150 nm. (e) Rotational power spectra of the three main classes (mean ± SEM is displayed). (f) Example of a polysome formed by three ribosome cliques connected by naked RNA filaments after GraFix cross-linking. Ribosome cliques are displayed using the same height scale color used in Fig. 6, with ribosomes in yellow (full Z-scale = 20 nm) and the RNA connecting the ribosome cliques in magenta. In the right panel, the cross-section height profile of the naked RNA (yellow line in the left panel) is shown.

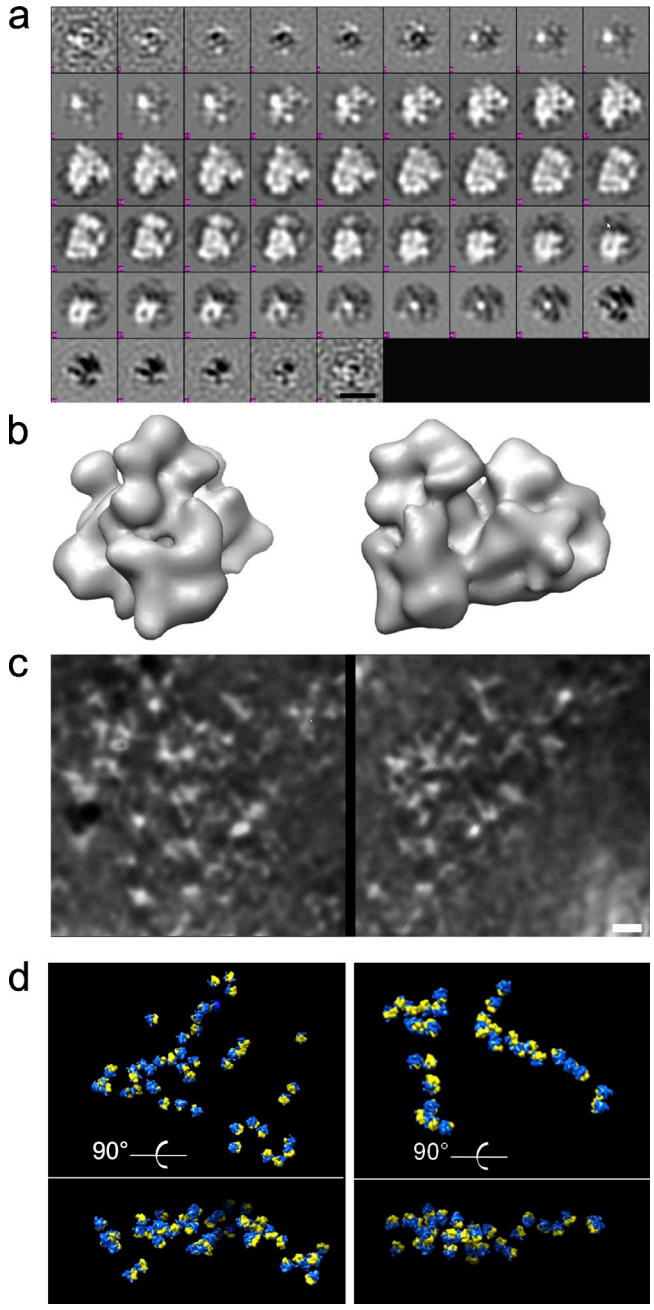

Figure S4. **Cryo-EM and cryo-ET ribosome and gallery of polysomes.** (a) Slices of the consensus polysomal monosome that demonstrate visualization of individual 80S complexes within polysomes with weaker satellite density deriving from variable translation factor stoichiometry. (b) Orthogonal views of the human ribosome reconstruction determined by projection matching assignment of orientations to the individual ribosomes within the small polysomes imaged. The resolution of the map is 55 Å. (c) Two sections from a cryo-electron tomogram of polysomes. (a and c) Bars: (a) 180 Å; (c) 50 nm. (d) Examples of two areas of cryo-tomograms that have been fitted with a template 80S map filtered to 60-Å resolution. Yellow, small subunit; blue, large subunit.

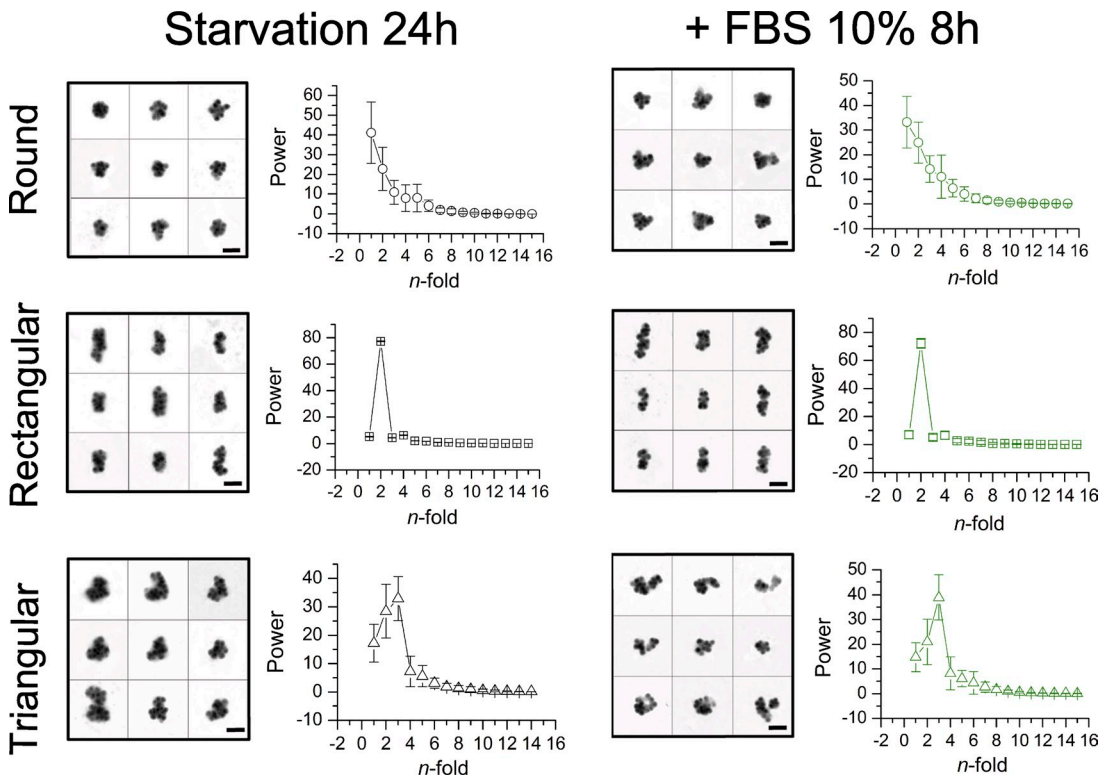

Figure S5. **RSC of polysomes after serum starvation and 10% FBS addition.** Comparison between galleries of HMW polysomes after serum starvation and serum readdition for 12 h is shown in the left panels. Bars, 100 nm. After grouping the 2D rotational spectra images, the differences in rotational symmetry for distinguishing classes are shown. In the right panels, the rotational power spectra for the most populated SOM classes of starved and FBS-treated polysomes (mean ± SD) are displayed. The objects considered for classification are 496 and 484 for the serum-starved and FBS-treated samples, respectively.

Table S1. **Comparison of AFM size values**

Parameter	80S		LMW	MMW	HMW
	Liquid	Air			
	nm	*nm*	*nm*	*nm*	*nm*
Height					
Peak 1	12.7 ± 1.5	6.0 ± 1.0	6.1 ± 1.5	6.4 ± 1.3	-
Peak 2	18.5 ± 2.5	9.1 ± 1.2	10.7 ± 1.7	11.6 ± 1.5	12.5 ± 2.7
Peak 3	-	-	-	-	15.8 ± 1.7
Width					
Peak 1	33.4 ± 3.7	34.1 ± 3.9	35.6 ± 3.7	32.6 ± 4.6	33.8 ± 4.9
Peak 2		-	56.8 ± 8.3	61.8 ± 8.3	88.9 ± 20.3
Length					
Peak 1	40.5 ± 7.1	42.2 ± 6.7	43.4 ± 5.4	38.9 ± 4.6	40.3 ± 7.0
Peak 2	-	-	74.3 ± 9.3	84.4 ± 15.2	124.7 ± 34.2
Peak 3	-	-	-	-	210.4 ± 42.9
Aspect ratio					
Peak 1	1.26 ± 0.07	1.19 ± 0.07	1.19 ± 0.07	1.26 ± 0.12	1.19 ± 0.06
Peak 2	1.48 ± 0.16	1.37 ± 0.11	1.37 ± 0.13	1.53 ± 0.23	1.37 ± 0.06
Peak 3	-	-	1.71 ± 0.21	-	1.54 ± 0.17
Peak4	-	-	-	-	1.92 ± 0.31

The distribution of size values (height, length, and width) for 80S in liquid and air and LMW, MMW, and HMW polysomes was obtained from bearing grain analysis (Gwyddion software). Each distribution was fitted with one or more Gaussians curves, giving the mean ± SEM size values that are listed in the table.

Video 1. **Gallery of 3D collection of composite polysomes with naked RNA.** Composite polysomes acquired with AFM and rendered with a ray-tracing software as 3D objects. Polysomes show subclusters of ribosomes (yellow) connected by ribbons (magenta). The color scheme matches that used in Fig. 6 (0–0.5 nm gray, 0.5–2 nm magenta, and 2–10 nm yellow).